Clinical Images and Case Reports

Received 8 May 2024 | Revised 10 May 2024 | Accepted 28 May 2024 | Published Online 8 Jun 2024

Published By: Vision Publisher

CICR 02 (6), 52-62

ISSN 2942-0776

Original Article

X-Ray Fluorescence Computed Tomography Imaging of Nanoparticles and Recent Advances in Biomedical X-ray Fluorescence Imaging

Muhammad Saeb Hashim[1], Range Faridoun Shafiq[2], Suz Ibrahim Mohammed[3], Ahmed Nouri Bakr[4]

[1,2,3,4]Kirkuk University, College of Science, Department of Physics, Iraq

Abstract:- There are a number of well-established methods in both preclinical and clinical uses of X-rays for non-invasive imaging, including computed tomography and tomographic imaging. Quantitative mapping of various elements in samples of interest is made possible by X-ray fluorescence analysis, while projection radiography offers anatomical information. So far, the technique has mainly found use in the material, archaeological, and environmental sciences for elemental identification and quantification; however, the application in the life sciences has been severely constrained by intrinsic spectral background problems that arise in larger objects. Multiple Compton-scattering events in the target objects provide this background, which severely restricts the minimum detectable marker concentrations that may be achieved. In this article, we take a look back at X-ray fluorescence imaging's (XFI) past, present its current and future promising preclinical applications, and predict its eventual clinical translation, which will be possible by lowering the aforementioned intrinsic background using specialised algorithms and new X-ray sources.

Monochromatic synchrotron x-rays are used in conventional x-ray fluorescence computed tomography (XFCT) in order to simultaneously find the concentration and spatial distribution of different elements, such metals, in a sample. It would appear, however, that in a conventional laboratory environment, the synchrotron-based XFCT method is not appropriate for in vivo imaging. To the best of our knowledge, our study is the first to show that XFCT imaging of a small object (about the size of an animal) with low concentrations of gold nanoparticles (GNPs) employing x-rays from the polychromatic diagnostic energy range is possible. To be more precise, we built a polymethyl methacrylate (PMMA) phantom that resembles a small animal's internal organs and tumours by filling two cylindrical columns with saline solution containing 1 and 2 weight percent (wt) GNPs, respectively. After suitable x-ray beam filtering and detector collimation, the phantom was scanned using an XFCT under a pencil beam geometry with a microfocus 110 kVp x-ray beam and a cadmium telluride (CdTe) x-ray detector. With contrast levels inversely proportional to gold concentration, the two GNP-filled columns were clearly visible in the reconstructed images. However, scanning duration is a major reason why the present pencil-beam implementation of XFCT is impractical for commonly used GNPs in in vivo imaging tasks. However, it is still possible to see things smaller than the current phantom size using a combination of several detectors and a small number of projections. The present study proposes various ways to alter the existing XFCT configuration, including using a quasi-monochromatic cone/fan x-ray beam and XFCT-specific spatial filters or pinhole detector collimators, to determine whether a bench-top XFCT system is feasible for GNP-based preclinical molecular imaging systems.

Keywords: X-Ray Fluorescence, Imaging, Nanoparticles, Biomedical X-ray

Corresponding Author: Muhammad Saeb Hashim†, Kirkuk University, College of Science, Department of Physics, Iraq

Introduction:

Wilhelm Conrad Röntgen famously discovered X-rays in 1895 [1]. Since then, many different kinds of X-ray imaging have emerged, all with the same goal of non-invasively revealing information about living things. Parts 1 and 2. In 1896, the idea of X-ray radiography was first put into clinical use, showing that X-ray imaging could be used for even soft tissue by the injection of a contrast liquid. Along with the fast development of new uses, many scientists toiled to improve the foundational X-ray technology, such as by making electron beams more precisely focused or by fine-tuning the quality of fluorescing screens to obtain higher-quality images [1-3]. Although the majority of these initial imaging techniques were based on the idea that materials with various densities transmit X-rays in different ways, leading to visual contrast, Max von Laue found the principle of X-ray diffraction by crystals in 1912. William Henry Bragg and his son William Lawrence Bragg established two new areas of study, X-ray crystallography and X-ray spectroscopy, after verifying the diffraction discovery using a different approach [4, 5]. Since then, X-ray crystallography has developed into a leading technique for determining the three-dimensional structure of proteins, a piece of data crucial for understanding how proteins work at the molecular level. There are still a number of challenges to structural protein determination, such as the need for big, well-diffracting crystals and the instability of purified proteins. However, these can be overcome with the help of new methods and strategies that have emerged in the last ten years [6-8]. When it comes to identifying features seen in imaging systems, X-ray spectroscopy has joined crystallography as an indispensable tool for getting data on local constituents.

Tomographic imaging has been a game-changer for medical research and science since Hounsfield found the Radon transform's practical uses in the middle of the twentieth century. Medical professionals and engineers now have a nondestructive and invasive way to get detailed pictures of the inside of a person or object thanks to X-ray computed tomography (CT) scans. We can now follow chemical tracers inside a living thing with the use of emission tomography scans like positron emission tomography (PET) and single-photon emission computed tomography (SPECT). With nanoparticles discovering so many uses in biomedicine, a tomographic imaging technique that can capture their distributions in living organisms could be useful in creating new diagnostic or therapeutic nanoagents [9, 10].

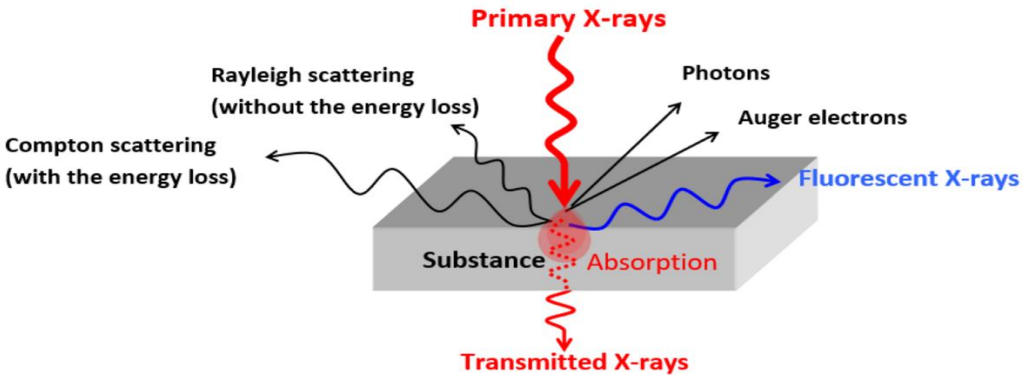

Figure 1. Interaction of X-rays with a substance

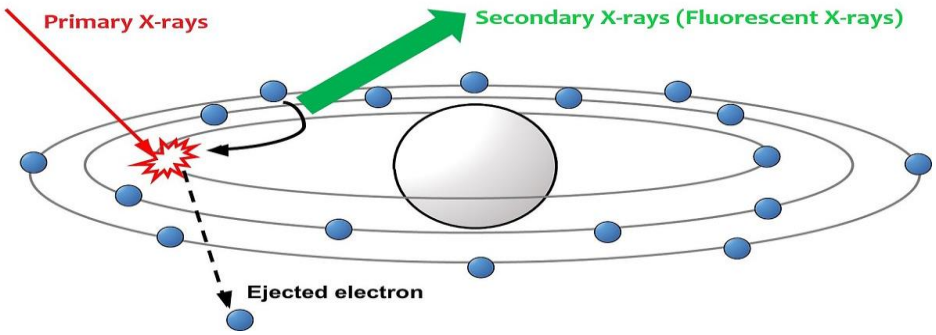

Figure 2. Principle of Fluorescent X-rays Emission

Transmission scans and emission scans are the two main types of tomographic imaging procedures. One common use of transmission scanning, like x-ray computed tomography (CT), is to construct a map of attenuation inside an item. This map can then be used to create an image of the object's structure or anatomy by differentiating between regions, such as bone, muscle, and fat. Radiation released by tracers that are injected or introduced into an item can be detected and localised by emission scanning [11]. When applied to live subjects, these tracers can be tailored to target specific areas of the body based on their chemical or biological composition; this allows for the generation of functional pictures illustrating various biological processes.

The use of emission tomography in radiology has been quite fruitful for quite some time. To provide a tomographic picture of what's going on inside an object, this method often uses radiation released by the material to be detected. Radioisotopes are the most common type of substances used in these types of scans; they can generate a single photon (SPECT) or two photons (PET) after positron annihilation. The 140-keV photon in 99mTc SPECT and the twin 511-keV annihilation photons in PET are examples of radioisotope-specific radiation that must be detected in order for this imaging modality to work [12, 13]. An alternative to directly injecting radioactive material is to capture photons that have been triggered by an external radiation beam; this allows for the reconstruction of images. Sputtered emission tomography is one name for these kinds of imaging techniques. Proton radiation dosage verification using PET imaging to identify 11C and 15O generated during proton interactions with tissue is one example. The detection of distinctive fluorescence x-rays generated from an item under irradiation by an external x-ray beam is the basis of x-ray fluorescence computed tomography (XFCT), which is based on it.

Problems with nanoparticle imaging

Because nanoparticles can have so many different characteristics, they provide a versatile platform for functional imaging. These characteristics may originate from the functional substance connected to the nanoparticles or be intrinsic to the nanoparticles themselves. Nanoparticles with a tiny enough size can enter the tumor's blood vessels and interstitium, leading to a higher concentration of nanoparticles in the tumour than in normal tissue. This process is called increased permeability and retention. Another option for "active" targeting is to attach nanoparticles to antibodies that detect tumor-specific biomarkers.

Possible targets include angiogenesis mediators like vascular endothelial growth factor and tumour indicators like epidermal growth factor receptor and human epidermal growth factor receptor-2 [14]. In a manner analogous to 18F deoxyglucose positron emission tomography (FDG-PET) imaging, metabolic agents like deoxyglucose can also be employed to actively target and internalise nanoparticles.

This book covers a lot of ground, including some of the more recent significant uses of nanoparticles in cancer imaging, radiation treatment, and thermal therapy. An integral part of the growth of these uses has been imaging, both in a laboratory setting and in living organisms. So far, it seems like the many imaging issues related to in vitro investigations have been successfully addressed. However, prior studies frequently ran into roadblocks or were postponed due to the absence of a reliable imaging technique or in vivo test to ascertain the bio-distribution of nanoparticles administered to animals [15]. In the absence of this instrument, the bio-distribution may only be ascertained by means of post-mortem study conducted on animals. If an imaging technique could quantify the spatial distribution and amount of nanoparticles within a tumour and other essential organs, it would be feasible to estimate the bio-distribution of nanoparticles in vivo.

Imaging using X-Ray Fluorescence

Fluorescence x-rays, also known as characteristic x-rays, are a distinctive physical property of metallic nanoparticles that can be directly controlled by their base material. Therefore, fluorescence x-rays are an effective method for determining a sample's chemical make-up. Each atom's electrons occupy a distinct energy level in the electron shell model. By absorbing or emitting a photon with an energy equal to the difference between their shells, electrons can move between these energy levels [16]. For any value of Z, there are distinct arrangements of these energy levels caused by differences in the nucleus charge. Therefore, the fluorescence x-ray energies that each atom emits are a reliable way to identify it, and these values are unique for each element.

When trying to determine what materials make up a sample, analytical methods that make use of fluorescence x-rays are frequently employed. Methods like energy-dispersive x-ray spectroscopy, which uses electrons in a way similar to

electron microscopy, and x-ray fluorescence, in which the material is assaulted with photons, are examples of such techniques in practice. Combining these technologies with tomographic imaging techniques allows XFCT to pinpoint the exact location and concentration of a fluorescing material inside an object. The following is a summary of the approach:

1. A photon beam is used to irradiate an object that has nanoparticles put onto it, causing it to emit fluorescence x-rays.

2. The energy of the fluorescence x-rays can be determined by an energy-sensitive photon detector device, which allows for the identification of the nanoparticles' base material.

3. tomographic reconstruction methods determine the nanoparticle distribution by analysing the intensity of the fluorescence signal at various locations and angles with respect to the object.

New Methods for Measuring X-Ray Fluorescence

With an emphasis on linking metal element abundance with monitoring of highly exposed employees, the methods have been enhanced since the 1970s to also permit determination of cadmium, lead, mercury, platinum, and gold. Because the item absorbs the transmitted characteristic radiation, X-ray fluorescence analysis could only be used in in vivo settings for elements with atomic numbers greater than about 40 in 1980. Those initial in vivo measurement setups contrasted various radionuclide sources, radiation sources, and X-ray tubes, and the radiation emitted was detected using Ge (Li)-detectors in conjunction with a collimator placed in front of the detector. The X-ray fluorescence spectra of lead in water measured with 57Co sources revealed a significant background level, primarily due to scattered primary photons, and thus revealed limits in the least detectable concentration. With X-ray tubes and specialised filters, it would be possible to attain minimum detectable concentration values that are comparable. The studies that were reported, however, only involved human fingerbones. It is stated that due to the low sensitivity of X-ray fluorescence measurements taken in vivo, it is not feasible to conduct detailed studies of the distribution of lead in the skeletons of people who are exposed to lead on the job. In its place, X-ray fluorescence analysis—which requires invasive procedures—is recommended for use with autopsy samples [17, 18]. The sensitivity is highly dependent on the tissue layer between the detector and the kidney surface, and the measurements primarily reflect the concentration in the kidney cortex instead of the whole organ. This was determined by studying the minimal detectable concentration of cadmium using a kidney model placed in water. To obtain the least background, an improved approach uses photons that are partly polarised and a detection angle of 90◦. The scattered beam is made more monoenergetic and the absorbed dose to the patient is reduced by using a modified X-ray therapy tube in conjunction with rods and foils. The patient sits on a specially designed chair during the procedure. Before taking fluorescence measurements, an ultrasound is used to localise the kidneys. To minimise background counts, collimated detectors with thick Si (Li) or Ge sensors face perpendicular to the main and dispersed beams. In order to further reduce the detection limit, optimisation efforts often involve increasing the measurement period and making use of an X-ray tube, which primarily emits radiation with a high fluence rate [19, 20]. The X-ray source, geometry, and measurement sensitivity were all thoroughly discussed. The three primary considerations that influence the selection of the photon source are as follows: (1) achieving an optimal penetration depth, (2) minimising the spectral background in the lead signal region, and (3) maximising the lead X-ray fluorescence yield per incident photon. Since Compton-scattered photons are known to be the primary background source, it is crucial that the Compton scatter peak be located as far away from the target lead X-ray peaks as feasible. To minimise the energy range and intensity of the observed Compton-scattered photons and to optimise the field of view and limit needless doses to the subject, 109Cd is chosen as the source with the optimal parameters, in conjunction with a unique collimator design. To account for differences in object size, shape, and overlying tissue thickness, the estimates propose normalising the detected lead counts to the coherent scatter peak (i.e., from Rayleigh scattering). This is based on the assumption that Compton scattering is isotropic in the laboratory system. Along with lead content measurements in exposed individuals, X-ray fluorescence was used to follow cisplatin in vivo, a cytostatic drug that has been effective in treating cancer. The background contribution from incoherently scattered (Compton) photons is reduced to about 40% compared to unpolarized radiation in this study using a measurement setup for plane-polarized photons, where the main beam is scattered in two mutually orthogonal directions at a target with a low atomic number but a high density [21, 22]. Just like in the other experiments that were discussed, the lowest concentration that can be detected at a depth of 4 cm for a duration

of 30 minutes is approximately 8 μg/g. Even at such low concentrations, the total mass of cisplatin in a human kidney is substantially more than in a mouse kidney, hence it is not possible to compare preclinical investigations with this marker concentration. While the 109Cd method has been widely used for a while, it cannot detect the trace amounts of lead that are found in the average person's blood. The new system was built by Nie et al. with the use of phantom experiments and Monte Carlo simulations. They anticipated that it would be around three times more sensitive than the conventional method.

Accurate Fluorescence Measurement

Imaging with X-Rays via Source and Detector Collimation

Even in its most basic form, XFCT allows one to pinpoint exactly where fluorescence x-rays come from. So, it's feasible to stimulate fluorescence x-rays in a very small area of an item utilising a pencil-thin x-ray beam. Subsequently, the fluorescence x-rays that were emitted along a line perpendicular to the initial x-ray beam are observed by a detector that is firmly collimated. This method involves repeatedly probing little areas of the item to find the concentration of nanoparticles in each [23, 24]. Figure 8.2 shows that this method is easy to implement, and reassembling the images is a breeze (because it doesn't require any understanding of tomographic techniques). Nevertheless, attenuation correction is increasingly tricky, and this approach has the drawback of not being able to gather more than one sinogram element per object irradiation, which increases scan times.

Experimenting with Collimated Fluorescent X-Rays from a Source or Detector

Modern techniques have made it possible to reduce scan times without sacrificing image quality. The observed fluorescence signal needs to be spatially recorded in some way so that a tomographic image of the nanoparticle distribution may be constructed. Measured signals for object-based image reconstruction methods based on inverting the Radon transform are line integrals. Radiation loss between the x-ray source and a single detector pixel is what transmission imaging is all about. If you want to use XFCT, you'll need to ensure that the fluorescence signal you detect follows a certain ray that goes through the item. Both the x-ray source and the detector are capable of accomplishing this. In the first scenario, known as source collimation, the incoming x-rays are focused into a narrow ray, also called a pencil beam, and the observed fluorescence signal is limited to following the path that this ray takes as it penetrates the material under study [25, 26]. The detector is positioned behind a parallel-pinhole collimator in the second scenario, known as detector collimation. So, the line that the detector's field of view follows through the object is the one from which the measured signal is derived. The ability to achieve extremely fine spatial resolution by producing a very narrow x-ray beam is one benefit of source collimation. Since each ray passing through the object needs to be irradiated independently, there is a trade-off between the beam width and the scan duration.

When conducting XFCT with a synchrotron beam to stimulate fluorescent x-rays inside the material, source collimation techniques are frequently used. Because of their high photon fluence and ability to be monochromatic, chromtron beams are ideal for XFCT. A high dose/signal ratio is characteristic of monochromatic beams (more on this later), and scan time is proportional to photon fluence. High resolution XFCT with manageable scan time can thus be achieved using synchrotron beams. A line or area detector records several rays through the object simultaneously, similar to SPECT imaging, which is achieved by detector collimation. As a result, all the data needed for a single projection may be collected at the same time, which is a huge time saver. Two of the constraints on in vivo XFCT imaging—the scan duration and imaging dose—can be reduced in this way. Nevertheless, the size of each detector pixel element becomes the limiting factor for the image's spatial resolution [27, 28]. Due to size constraints on energy-sensitive detectors, this can limit the image quality for small-animal polychromatic XFCT. To alleviate these issues, researchers are still working.

Evaluation of the XFCT Output

Within the item, the fluorescence detection process is impacted by two primary impacts. The first is the well-known phenomenon of fluorescence x-ray emission from nanoparticles. This happens when a photon from a source interacts with an atom in a nanoparticle, causing an electron shell vacancy and hence the emission of fluorescence x-rays. The second effect is the scattering of the source photons by the object's Compton surface. The XFCT signal is the first effect, while the noise is the scattered photons. To isolate the photons that really fluoresce from the ones that are distributed about the object, an energy-sensitive detector is required. Scatter correction is significantly more

challenging in XFCT due to its physics compared to other emission tomography modalities. Specific directional gamma tomography (SPECT) involves injecting a radioactive tracer into the patient's circulation and then using detectors strategically placed around the body to assess the radiation intensity in various directions. Since the energy of the tracer's produced photons can only be reduced by scattering and other effects at these energies [29–32], the patient's highest energy photons are those that have not interacted. A basic energy window that excludes lower energies allows scatter to be separated from the main.

Conversely, in XFCT, the x-ray source contains the photons with the maximum energy. The reason behind this is that photons that undergo fluorescence have lower energies compared to those that undergo photoelectric absorption in the atom from where they originated. The K and L edges of gold, for example, are at 80.7 and 11.9-14.4 keV, respectively. An 81 keV source photon will produce a 66 or 68 keV fluorescence photon for the significant Kα (L-to-K) fluorescence x-ray emission. An additional 66 keV photon might be produced by subjecting the identical 81 keV photon to Compton scattering at a right angle. As a result, using energy alone to distinguish between dispersed and fluorescence photons is not feasible [33]. At the fluorescence photon energies, you need to subtract an estimated value for the scatter background from the recorded signal. Picking the right x-ray source energy spectrum is crucial for efficient XFCT data gathering. More specifically, the selected energy shell of the nanoparticles must be excited to its fullest potential, and this requires an optimised spectrum. Think about the K-shell that a piece of gold has. Any photon projected onto a gold atom with the intention of eliciting K-shell fluorescence x-ray emission must surpass the 81 keV binding energy of the two innermost electrons. The maximum number of fluorescence photons would be emitted by a monoenergetic beam of 81 keV photons because the interaction cross section of gold is 81 keV (due to K-shell photoelectric absorption).

If a monochromatic beam is not available, XFCT can still be carried out using a polychromatic beam. However, in order to harden the beam spectrum, ordinary bremsstrahlung-heavy photon beams require extensive x-ray filtering. It is pointless to increase dose and noise when a photon is below the nanoparticles' desired absorption edge [34, 35] because it cannot trigger fluorescence x-ray emission. In order to image areas filled with gold nanoparticles (GNPs) inside tiny objects the size of animals, with the Kα fluorescence line as the goal, the x-ray beam should be focused as much as possible above 81 keV. The decrease in the source's photon fluence rate caused by extensive filtration is an issue since it increases the scanning time needed to obtain a usable image. Therefore, it is necessary to strike a balance between source spectral hardness, x-ray dose, and photon fluence when developing an appropriate x-ray filter for polychromatic XFCT. Lead, a filtering material for certain GNP-based XFCT applications, produces an x-ray beam with a 110 kVp peak between 50 and 90 keV due to its transmission band that spans the L and K shells (16-88 keV). The poor signal-to-dose ratio is caused by the reduced transmission above 90 keV and the high fluence below 80 keV, yet this is still acceptable for GNP-based XFCT. Nanoparticles with an atomic number between 50 (tin) and 70 (ytterbium) are most suited for XFCT applications that use a lead-filtered beam.

The stacked layers of tin, copper, and aluminium that make up the Thoraeus filter are one type of x-ray filter that had uses during the days of orthovoltage radiation therapy. The spectra emitted by this filter exhibit a sharp peak in the 90- to 100-keV band for x-rays with a power range of 100- to 150-kVp. Nevertheless, the overall fluency is much diminished. The quasi-mono-chromatization of a polychromatic beam is an additional strategy that could be considered. When dealing with beam energies greater than 50 keV, when filtration becomes problematic, a material like highly oriented pyrolitic graphite (HOPG) can be used to extract a single energy from a beam [36, 37]. The homogenous interatomic spacing and densely packed crystal structure of HOPG make it possible to use Bragg diffraction to extract a monochromatic beam. It is theoretically possible to separate a 95 keV beam from a polychromatic one with a scattering angle of about 1°. The low intensity of the resulting pencil beam or the geometrical intricacy of employing Bragg diffraction to produce a fan/cone beam are some practical concerns that would make it challenging to apply this technology to GNP-based XFCT.

It is necessary to isolate the fluorescence peak from the Compton scatter background in order to calculate the fluorescence signal strength. The difference between the discrete energies at which fluorescence x-ray emission happens and the continuum spectrum at which Compton scattered photos appear makes this a real possibility. Because of the relatively large scatter-to-primary ratio of a polychromatic beam, an energy-sensitive detector with respectable energy resolution is necessary. It is possible to calculate the fluorescence intensity by fitting a polynomial to the

scatter background, provided that a decent signal is also obtained for the adjacent energy channels surrounding the fluorescence peak. This task is effectively handled by a third-degree polynomial [38, 39] for gold Kα fluorescence photons produced using a lead- or tin-filtered polychromatic beam. You might get away with a lower-order fit for other energies or spectra. Utilising more sophisticated methods of curve fitting or spectrum filtering can potentially yield an improved signal.

Synchrotron X-Flexible Charge Transfer Technology: Advancements and Uses

The utilisation of a synchrotron as an x-ray source has been the backbone of nearly every XFCT application. The rapid acquisition of XFCT data with a low SPR is made possible by the extremely bright and monochromatic synchrotron x-ray beams, as indicated earlier in the section. It was only logical to expand the use of x-ray fluorescence techniques to tomography, as researchers had been doing so for some time to determine a sample's material composition.

The detection of already-used x-ray contrast ants, including gadolinium and iodine, was the primary focus of much of the early work on synchrotron XFCT for biological applications. Imaging of cerebral blood flow with 123I isotopes is another application of iodine for SPECT. For XFCT studies, these high-Z contrast agents made perfect sense because the detection of a fluorescence signal is dependent on the energy [40] of the emitted fluorescence photon. The capacity to detect far lower amounts of iodine using x-ray fluorescence gives XFCT an edge over transmission CT, which is utilised for detecting extremely high concentrations of contrast agents in blood. Iodine Kα rays can only penetrate small objects due to their narrow penetration depth. As early as 1989, Cesareo and Mascarenhas published a proof of concept for fluorescence tomography. As mentioned earlier in this chapter, they did not rely on inversion of the Radon transform as their method. Instead, they measured each voxel in their sample directly by collimating the x-ray source and detector. They showed that fluorescence tomography can localise high-Z compounds within an object non-destructively by imaging a 2 × 2 cm2 plexiglass object with regions loaded with iodine at a concentration of 5 mg/mL. This was done as a proof-of-principle. Iodine concentrations as low as 50 ng/mL were also detected in a 1995 publication by Takeda et al., who conducted a comparable study.

It was challenging to account for attenuation in the "direct measurement" geometry, according to one of the investigations cited earlier. Each neighbouring pixel's tracer concentration determined the signal attenuation in that pixel. By adding the attenuation along the lines from pixel-to-source and pixel-to-detector, the pictures were adjusted. This meant that any mistake in one pixel would affect all pixels behind it. To solve this problem, Hogan et al.[41] conducted computer simulations to demonstrate that XFCT images may be reconstructed using rotational tomography and the source collimation geometry. This appeared in 1991. A 5-mm-diameter phantom containing iodine at concentrations ranging from 0.2 to 2 mg/mL was imaged using Fourier back-projection.
Using an experimental setup that depended on an iterative reconstruction procedure to generate an image, Rust and Weigelt (1998) once again proved the applicability of Radon inversion for XFCT two years later. They managed to obtain pictures of iodine within a 1.5-cm ex vivo thyroid gland at concentrations of 0.6 mg/mL by applying their technology to conduct imaging of a biological material. In 1999, Takeda et al. measured thyroid function similarly.

Benchtop XFCT

Synchrotron beams are unquestionably well-suited for XFCT due to their high fluence rates and wide energy spectra. Problems arise when using synchrotron beams, however, and this is particularly true when imaging living organisms. The difficulty in obtaining a synchrotron beam makes imaging with one a challenging task. Nearly forty synchrotron facilities are active at this time, supporting studies in biology, physics, chemistry, and materials science, among other relevant fields [42, 43]. The enormous expense of constructing a synchrotron facility makes it unusual for any level of government lower than the federal or state to run one. Finally, synchrotron x-rays are hard to come by due to the finite amount of beam lines. On top of that, regular in vivo imaging of animals may be too risky with the usual dose rates of high-flux synchrotron beams.

Given the reasons mentioned above, it would be advantageous to be able to conduct XFCT in a laboratory benchtop environment. Benchtop polychromatic XFCT is still in its infancy as a field, and its practical applications are limited thus far. Nonetheless, this XFCT method has shown its strength and adaptability in a number of proof-of-principle investigations. The exceedingly high SPR is the primary obstacle to XFCT when using a polychromatic source. An example would be a sample loaded with low concentrations of GNPs emitting less fluorescence photons compared to a

lead-filtered 110 kVp beam, which can result in a Compton scattering number that is over a hundred times greater.

It is crucial to think about how to prevent the creation or detection of scattered photons before attempting to obtain a fluorescence signal using a polychromatic beam. Think of a spectrum that doesn't exist. Overlapping a flat background of scattered photons is the idealised fluorescence peak shown by the solid line. It would be easy to separate the fluorescence peak's height from the scatter background if a detector could measure this spectrum for an infinitely long time [44]. Acquiring a usable signal while exposing the individual to as low dosage as feasible is essential for any realistic imaging technique. Until the end of time exists for counting. There will be oscillations from channel to channel with a magnitude of around $\sqrt{N}$, according to the Poisson model of counting statistics, for a scatter background of magnitude N. Accurate measurement of the fluorescence signal requires a peak height greater than this amount.

The development of a fluorescence signal robust enough to withstand variations in the scatter background at low concentrations of GNPs is thus a significant obstacle to benchtop XFCT. This can be achieved by selecting the x-ray filter and acquisition geometry with precision. Even so, it's still a big drawback, and trying to get around it by obtaining the signal for a longer duration can increase the acquisition time and x-ray dose.

An picture of GNPs with low concentrations (<2% by weight) was successfully acquired in 2010 by Cheong et al. using a 110-kVp tabletop x-ray source. The experiment was carried out in a PMMA phantom with a diameter of 5 cm while a lead-filtered pencil beam was used to measure the amount of Kα fluorescence photons generated by GNPs in order to calculate the gold concentration [45, 46]. Several synchrotron-based investigations included source collimation in their fluorescence acquisition geometry, but this one additionally included a weak detector collimator and features from the direct measurement geometry. A rather broad collimator was used to shield a cadmium telluride (CdTe) detector, which was positioned at a right angle to the pencil beam's centre axis. This allowed the detector to see a field of view within the phantom that was approximately 1 cm in diameter. The detector was moved in five 1-cm increments for every pencil beam that passed across the item [47]. After subtracting the Compton noise from the observed fluorescence spectra at each step, the five-step response was added up to form each line projection. A priori knowledge of the geometry informed the manual scatter correction that was a part of the unfiltered back-projection process used to reconstruct the image.

CONCLUSION

The atomic structure makes fluorescence x-rays a potent tool for determining a sample's material composition. XFCT is a technique that uses tomographic image reconstruction methods in conjunction with x-ray fluorescence analysis to determine the concentration and position of metallic nanoparticles like GNPs in living organisms. These objectives may be attainable for GNPs in small animals at extremely low concentrations using a tabletop equipment with additional improvements. For biomedical researchers dealing with nanoparticles, this kind of technology would unlock a treasure trove of new analytical tools.

When it comes to the minimal detectable signal and its use in many fields, X-ray fluorescence imaging has come a long way since its initial use in the late 1970s. Modern setups can be realised at synchrotrons or conventional X-ray sources, allowing for much higher precision monitoring and control of the radiation dose and applied beam diameters, in contrast to the first studies that primarily used radioactive isotopes and special geometric configurations. Although X-ray fluorescence imaging's viability for both preclinical and clinical use was questioned in the early 2000s, the modality has seen remarkable development to enhance its capabilities in the last several years. Measurements at existing X-ray systems have been made possible by developing compact setups, and various methodologies have been developed to address fundamental background restrictions. Detecting low marker concentrations in huge objects is now possible with the use of pixelated detectors, collimators, pinholes, or specific filters; this definitely lays the way for future therapeutic applications. Measurements with the utmost sensitivity are now only possible at synchrotron beamlines, which severely restricts the possible uses. Consequently, it is critical to create more compact systems that would enable the modality to be used in clinical and laboratory settings. There are a variety of approaches to developing small X-ray systems, but the majority of them integrate XFI and CT imaging to get functional and anatomical data simultaneously. To have the best spatial resolution and detection sensitivity, these systems now struggle with the requirement to concentrate and monochromatize the incident radiation from a standard X-ray tube.

There is a need for improvement in the efficiency of dedicated X-ray optics in order to assess acceptable imaging periods and radiation doses, but they do provide a potential solution by focusing a given X-ray energy of interest. In general, XFI has a wide range of potential uses, including elemental distribution measurements in non-destructive testing, investigating the uptake of specific entities into single cells, and various medical imaging applications, such as studying the biodistribution of novel medicinal drug compounds or accurately localising tumours. Hence, XFI has the ability to supplement other established molecular imaging methods in areas where XFI provides unique data, such as the high-resolution, sensitivity, and simultaneous in vivo tracking of multiple immune cell subtypes in preclinical studies.

REFERENCES

1. Cherry, S., J. Sorenson, and M. Phelps. 2003. Physics in Nuclear Medicine, 3rd edn. Philadelphia, PA: Saunders. Copland, J. A., M. Eghtedari, V. L. Popov et al. 2004. Bioconjugated gold nanoparticles as a molecular based contrast agent: Implications for imaging of deep tumors using optoacoustic tomography. Molecular Imaging and Biology 6:341–349.
2. de Jonge, M. D., and S. Vogt. 2010. Hard x-ray fluorescence tomography— an emerging tool for structural visualization. Current Opinion in Structural Biology 20:606–614.
3. El-Sayed, I., X. Huang, and M. El-Sayed. 2005. Surface plasmon resonance scattering and absorption of anti-EGFR antibody conjugated gold nanoparticles in cancer diagnostics: Applications in oral cancer. Nano Letters 5:829–834.
4. Hogan, J. P., R. A. Gonsalves, and A. S. Krieger. 1991. Fluorescent computer tomography: A model for correction of x-ray absorption. IEEE Transactions on Nuclear Science 38: 1721–1727.
5. Jones, B. L., and S. H. Cho. 2011. The feasibility of polychromatic cone-beam x-ray fluorescence computed tomography (XFCT) imaging of gold nanoparticle-loaded objects: A Monte Carlo study. Physics in Medicine and Biology 56:3719–3730.
6. Lange, K., and R. Carson. 1984. EM reconstruction algorithms for emission and transmission tomography. Journal of Computer Assisted Tomography 8:306–316.
7. Li, J., A. Chaudhary, S. J. Chmura et al. 2010. A novel functional CT contrast agent for molecular imaging of cancer. Physics in Medicine and Biology 55:4389–4397.
8. Liu, C.-J., C.-H. Wang, C.-L. Wang et al. 2009. Simple dose rate measurements for a very high synchrotron x-ray flux. Journal of Synchrotron Radiation 16:395–397.
9. Maeda, H., J. Fang, T. Inutsuka, and Y. Kitamoto. 2003. Vascular permeability enhancement in solid tumor: various factors, mechanisms involved and its implications. International Immunopharmacology 3:319–328.
10. McNear, D. H., E. Peltier, J. Everhart et al. 2005. Application of quantitative fluorescence and absorption-edge computed microtomography to image metal compartmentalization in Alyssum murale. Environmental Science & Technology 39:2210–2218.
11. Mukherjee, P., R. Bhattacharya, N. Bone et al. 2007. Potential therapeutic application of gold nanoparticles in B-chronic lymphocytic leukemia (BCLL): Enhancing apoptosis. Journal of Nanobiotechnology 5:4.
12. Oelfke, U., G. K. Y. Lam, and M. S. Atkins. 1996. Proton dose monitoring with PET: Quantitative studies in Lucite. Physics in Medicine and Biology 41:177.
13. Pereira, G. R., R. T. Lopes, M. J. Anjos, H. S. Rocha, and C. A. Pérez. 2007. X-ray fluorescence microtomography analyzing reference samples. Nuclear Instruments and Methods in Physics Research Section A 579:322–325.
14. Rocha, H. S., G. R. Pereira, M. J. Anjos et al. 2007. Diffraction enhanced imaging and x-ray fluorescence microtomography for analyzing biological samples. X-ray Spectrometry 36:247–253.

15. Rust, G. F., and J. Weigelt. 1998. X-ray fluorescent computer tomography with synchrotron radiation. IEEE Transactions on Nuclear Science 45:75–88.

16. Shepp, L., and Y. Vardi. 2007. Maximum likelihood reconstruction for emission tomography. IEEE Transactions on Medical Imaging 1:113–122.

17. Takeda, T., M. Akiba, T. Yuasa et al. 1996. Fluorescent x-ray computed tomography with synchrotron radiation using fan collimator. Medical Imaging 1996: Physics of Medical Imaging 2708:685–695.

18. Takeda, T., J. Wu, Q. Huo et al. 2009. X-ray fluorescent CT imaging of cerebral uptake of stable-iodine perfusion agent iodo-amphetamine analog IMP in mice. Journal of Synchrotron Radiation 16:57–62.

19. Takeda, T., Q. Yu, T. Yashiro et al. 1999. Human thyroid speci- men imaging by fluorescent x-ray computed tomography with synchrotron radiation. Medical Imaging 1996: Physics of Medical Imaging 3772:258–267

20. Eckert, M. Max von Laue and the discovery of X-ray diffraction in 1912. Ann. Phys. 2012, 524, A83–A85. [CrossRef] 3. Kermani, A.A.; Aggarwal, S.; Ghanbarpour, A. Chapter 11—Advances in X-ray crystallography methods to study structural dynamics of macromolecules. In Advanced Spectroscopic Methods to Study Biomolecular Structure and Dynamics; Academic Press: Cambridge, MA, USA, 2023; pp. 309–355.

21. Levin, E.R. Principles of X-Ray Spectroscopy. Scanning Electron Microsc. 1986, 1,

22. Koziej, D.; DeBeer, S. Application of Modern X-ray Spectroscopy in Chemistry—Beyond Studying the Oxidation State. Chem. Mater. 2017, 29, 7051–7053.

23. Kalender, W.A. Technical Foundations of Spiral CT. Semin. Ultrasound CT MR 1994, 15, 81–89.

24. Hussain, S.; Mubeen, I.; Ullah, N.; Shah, S.S.U.D.; Khan, B.A.; Zahoor, M.; Ullah, R.; Ali Khan, F.; Sultan, M.A. Modern Diagnostic Imaging Technique Applications and Risk Factors in the Medical Field: A Review. BioMed Res. Int. 2022, 2022, 5164970.

25. Frush, D.P.; Callahan, M.J.; Coley, B.D.; Nadel, H.R.; Guillerman, R.P. Comparison of the different imaging modalities used to image pediatric oncology patiens: A COG diagnostic imaging committee/SPR oncology committee white paper. Pediatr. Blood Cancer 2023, 70, S4.

26. Borges, A.P.; Antunes, C.; Curvo-Semedo, L. Pros and Cons of Dual-Energy CT Systems: “One Does Not Fit All”. Tomography 2023, 9, 195–216.

27. Wu, L.; Bak, S.; Shin, Y.; Chu, Y.S.; Yoo, S.; Robinson, I.K.; Huang, X. Resolution-enhanced X-ray fluorescence microscopy via deep residual networks. Npj Comput. Mater. 2023, 9, 43.

28. Körnig, C.; Staufer, T.; Schmutzler, O.; Bedke, T.; Machicote, A.; Liu, B.; Liu, Y.; Gargioni, E.; Feliu, N.; Grüner, F.; et al. In-situ X-Ray Fluorescence Imaging of the Endogeneous Iodine Distribution in Murine Thyroids. Sci. Rep. 2022, 12, 2903.

29. Manohar, N.; Reynoso, F.J.; Diagaradjane, P.; Krishnan, S.; Cho, S.H. Quantitative imaging of gold nanoparticle distribution in a tumor-bearing mouse using benchtop X-ray fluorescence computed tomography. Sci. Rep. 2016, 6, 22079.

30. Workman, R.B.; Coleman, R.E. Fundamentals of PET and PET/CT imaging. In PET/CT Applications in Non-Neoplastic Conditions; Springer: New York, NY, USA, 2011; Volume 1228, pp. 1–18.

31. Jenkins, R. X-ray Fluorescence Spectrometry; John Wiley & Sons, Inc.: Hoboken, NJ, USA, 1988. 15. Hoffer, P.B.; Jones, W.B.; Crawford, R.B.; Beck, R.; Gottschalk, A. Fluorescent thyroid scanning: A new method of imaging the thyroid. Radiology 1968, 90, 342–344.

32. Börjesson, J.; Mattsson, S. Toxicology; In vivo x-Ray Fluorescence For the Assessment of Heavy Metal Concentrations in Man. Appl. Radiat. Isot. 1995, 46, 571–576.

33. Cheong, S.-K.; Jones, B.L.; Siddiqi, A.K.; Liu, F.; Manohar, N.; Hyun Cho, S. X-ray fluorescence computed tomography (XFCT) imaging of gold nanoparticle-loaded objects using 110 kVp X-rays. Phys. Med. Biol. 2010, 55, 647–662.

34. Von Busch, H.; Harding, G.; Martens, G.; Schlomka, J.-P.; Schweizer, B. Investigation of externally activated X-ray fluorescence tomography for use in medical diagnostics. In Medical Imaging 2005: Physics of Medical Imaging; SPIE: Washington, DC, USA, 2005.

35. Grüner, F.; Blumendorf, F.; Schmutzler, O.; Staufer, T.; Bradbury, M.; Wiesner, U.; Rosentreter, T.; Loers, G.; Lutz, D.; Hoeschen, C.; et al. Localizing functionalized gold-nanoparticles in murine spinal cords by X-ray fluorescence imaging and backgroundreduction through spatial filtering for human-sized objects. Sci. Rep. 2018, 8, 16561.

36. Ungerer, A.; Staufer, T.; Schmutzler, O.; Körnig, C.; Rothkamm, K.; Grüner, F. X-ray-Fluorescence Imaging for In Vivo Detection of Gold-Nanoparticle-Labeled Immune Cells: A GEANT4 Based Feasibility Study. Cancers 2021, 13, 5759.

37. Moses, W.W. Fundamental Limits of Spatial Resolution in PET. Nucl. Instrum. Methods Phys. Res. Sect. A 2011, 648 (Suppl. S1), S236–S240.

38. Achterhold, K.; Bech, M.; Schleede, S.; Potdevin, G.; Ruth, R.; Loewen, R.; Pfeiffer, F. Monochromatic computed tomography with a compact laser-driven X-ray source. Sci. Rep. 2013, 3, 1313

39. Jacquet, M. High intensity compact Compton X-ray sources: Challenges and potential of applications. Nucl. Instrum. Methods Phys. Res. Sect. B 2014, 331, 1–5.

40. Powers, N.D.; Ghebregziabher, I.; Golovin, G.; Liu, C.; Chen, S.; Banerjee, S.; Zhang, J.; Umstadter, D.P. Quasimonoenergetic and tunable X-rays from a laser-driven Compton light source. Nat. Photonics 2014, 8, 29–32.

41. Ta Phuoc, K.; Corde, S.; Thaury, C.; Malka, V.; Tafzi, A.; Goddet, J.P.; Shah, R.C.; Sebban, S.; Rousse, A. All-optical Compton gamma-ray source. Nat. Photonics 2012, 6, 308–311.

42. Brümmer, T.; Debus, A.; Pausch, R.; Osterhoff, J.; Grüner, F. Design study for a compact laser-driven source for medical X-ray fluorescence imaging. Phys. Rev. Accel. Beams 2020, 23, 031601.

43. Bohlen, S.; Wood, J.C.; Brümmer, T.; Grüner, F.; Lindstrøm, C.A.; Meisel, M.; Staufer, T.; D'Arcy, R.; Põder, K.; Osterhoff, J. Stability of ionization-injection-based laser-plasma accelerators. Phys. Rev. Accel. Beams 2022, 25, 031301. [CrossRef] 33. Brümmer, T.; Bohlen, S.; Grüner, F.; Osterhoff, J.; Põder, K. Compact all-optical precision-tunable narrowband hard Compton X-ray source. Sci. Rep. 2022, 12, 16017.

44. Staufer, T. X-Ray Fluorescence Imaging with a Laser-Driven X-ray Source. Ph.D. Thesis, University of Hamburg, Hamburg, Germany, 2020.

45. Shaker, K.; Vogt, C.; Katsu-Jiménez, Y.; Kuiper, R.V.; Andersson, K.; Li, Y.; Larsson, J.C.; Rodriguez-Garcia, A.; Toprak, M.S.; Hertz, H.M.; et al. Longitudinal In-Vivo X-ray Fluorescence Computed Tomography with Molybdenum Nanoparticles. IEEE Trans. Med. Imaging 2020, 39, 12.

46. Dogdas, B.; Stout, D.; Chatziioannou, A.F.; Leahy, R.M. Digimouse: A 3D whole body mouse atlas from CT and cryosection data. Phys. Med. Biol. 2007, 52, 577.

47. Jung, S.; Kim, T.; Lee, W.; Kim, H.; Kim, H.S.; Im, H.J.; Ye, S.J. Dynamic In Vivo X-ray Fluorescence Imaging of Gold in Living Mice Exposed to Gold Nanoparticles. IEEE Trans. Med. Imaging 2020, 39, 526–533.